

Functional expression and cellular distribution of diastrophic dysplasia sulfate transporter (*DTDST*) gene mutations in HEK cells

Lawrence P. Karniski*

Laboratory of Epithelial Transport, Department of Internal Medicine, Veterans Affairs Medical Center and University of Iowa College of Medicine, Iowa City, IA 52242, USA

Received April 17, 2004; Revised and Accepted July 20, 2004

Defects in sulfate transport in chondrocytes lead to undersulfation of the cartilage extracellular matrix proteoglycans. Mutations in the diastrophic dysplasia sulfate transporter (*DTDST*) gene have been linked to four chondrodysplasias of varying severity. To characterize disease-causing mutations of *DTDST*, we expressed *DTDST*-mediated sulfate transport in mammalian HEK-293 cells and determined that the wild-type protein is glycosylated and localized to the cell plasma membrane. Four mutations, A715V, C653S, Q454P and R279W, stimulated sulfate transport at rates only 39–62% of wild-type *DTDST*. These four mutations were expressed on the plasma membrane of the cell, but the amount of expressed protein was reduced when compared with wild-type *DTDST*. The Q454P mutant is unique in that it is not properly glycosylated in HEK cells. There was no difference in sulfate transport activity between cells transfected with either the Δ V340 or the G678V mutations and control HEK cells. Furthermore, the G678V mutation is not expressed along the plasma membrane, but is trapped within the cytoplasm. When comparing the sulfate transport capacity of each *DTDST* mutation with the chondrodysplasia in which it has been identified, we find that individuals with severe achondrogenesis 1B phenotype have null mutations on both *DTDST* alleles. Heterozygotes for both a null mutation and a partial-function mutation result in either atelosteogenesis type 2 or DTD, whereas the milder, recessive multiple epiphyseal dysplasia phenotype is homozygous for partial-function mutations. In contrast to previous studies in *Xenopus laevis* oocytes, we find a strong correlation between the severity of the phenotype and the level of residual transport function in mammalian cells.

INTRODUCTION

The diastrophic dysplasia sulfate transporter (*DTDST*) gene was first described by Hästbacka *et al.* (1), and is a member of the SLC26A family of anion transporters (SLC26A2). The gene encodes a sulfate transporter that accepts chloride and possibly bicarbonate as substrates, and is inhibited by anion exchange inhibitors, including 4,4'-diisothiocyanostilbene-2,2'-disulfonic acid (DIDS) (2). Since its first description, over 30 mutations in *DTDST* have been described in four recessively inherited chondrodysplasias (reviewed in 3). Achondrogenesis 1B (ACG-1B) is the most severe form of these chondrodysplasias, resulting in skeletal underdevelopment and death preceding or shortly after birth (4). Atelosteogenesis type II (AO-II) can be lethal in the neonatal period (5), whereas diastrophic dysplasia (DTD) and autosomal recessive

multiple epiphyseal dysplasia (rMED) are considered to be the least severe forms (6–9). McAlister dysplasia has been described as a variant of AO-II (10), and broad bone-platyspondyly is a variant of DTD (11).

Reduced sulfate transport in chondrocytes of individuals with *DTDST* mutations results in undersulfation of proteoglycans and abnormal cartilage formation. Correlations between mutations in the *DTDST* gene and clinical phenotypes have been described (3,12). One possible explanation for the variations in disease severity between the chondrodysplasias is that the differences in residual sulfate uptake via the mutated *DTDST* sulfate transporter influence the severity of the phenotype (5). To test this hypothesis, several investigators have examined tissues from individuals with ACG-1B, AO-II and DTD (4,5,10,13–15). When compared with normal controls, a reduction in either sulfate uptake or proteoglycan sulfation

*To whom correspondence should be addressed at: Department of Internal Medicine, E300C, University of Iowa Hospitals, 200 Hawkins Drive, Iowa City, IA 52242, USA. Tel: +1 3193563971; Fax: +1 3193562999; Email: lawrence-karniski@uiowa.edu

has been detected in cells from every individual with a chondrodysplasia; however, a correlation between the severity of the disease and the level of sulfate transport or proteoglycan sulfation has not been found. Interpretation of these types of studies is difficult due to the availability of small number of patients with each phenotype and by the fact that pathways other than transport via DTDST may contribute to the sulfate pool in chondrocytes (10,16,17).

In a previous study, we expressed 11 different disease-causing *DTDST* mutations in *Xenopus laevis* oocytes and correlated the functional sulfate transport capacity at the molecular level with known genotype/phenotype relationships (18). When the sulfate transport function of the different *DTDST* mutations was grouped according to phenotypes, individuals with the most severe form (ACG-1B) tend to be homozygous for null mutations, individuals with the moderately severe AO-II have at least one allele with a loss of function mutation and individuals with the milder forms (DTD and rMED) typically are homozygous for mutations with residual sulfate transport function; however, the correlation between the residual transport function and the severity of phenotype was not absolute. For example, compound heterozygotes with a null mutation on one allele and a mutation with near-normal function in oocytes on the other allele have been identified in chondrodysplasias of all levels of severity. The inconsistent correlation between the residual transport function and the disease severity may be related to the fact that *X. laevis* oocytes process mutant proteins differently when compared with mammalian cells. In the present study, we have expanded upon these earlier results by determining the functional activity and cellular location of *DTDST* mutations following the expression in human cultured cells. The results presented here offer an explanation as to why some mutations have near-normal function in oocytes but result in clinical disease.

RESULTS

To test whether mutant DTDST proteins have similar functional activity when expressed in mammalian cells when compared with *X. laevis* oocytes (18), six *DTDST* mutants with partial function in oocytes, and four null mutations, were expressed in HEK-293 cells, and the rate of DIDS-inhibitable, sodium-independent sulfate transport was determined. HEK-293 cells were chosen for these studies because preliminary experiments showed that *DTDST* is not expressed in these cells, and they have a low level of endogenous DIDS-inhibitable, sodium-independent sulfate transport activity.

As shown in Figure 1, HEK cells transfected with wild-type *DTDST* had a rate of sulfate uptake five-fold greater than the control HEK cells transfected with vector minus the *DTDST* insert. This is consistent with the functional expression of a sulfate transport protein. Four mutations that had partial function in oocytes, A715V, C653S, Q454P and R279W, also have partial function in mammalian cells, with sodium-independent sulfate transport significantly greater than the controls. In contrast, two mutations with partial function in oocytes, Δ V340 and G678V, had sulfate uptake in HEK cells that was not significantly different than that in controls, demonstrating that Δ V340 and G678V are non-functional in HEK cells. We also tested four mutations, L483P, R178X, Δ a1751 and

N425D, that had no transport activity in oocytes. For each of these four mutations, sulfate transport activity following transfection in HEK cells was not significantly different than that in controls (data not shown), demonstrating that null mutations in oocytes are non-functional in mammalian cells as well.

To determine whether there are differences between the amount and the cellular location of expressed mutant DTDST, we generated monoclonal antibodies against intact, purified DTDST protein. As shown in Figure 2, immunoblots of homogenates of HEK cells transfected with *DTDST* show two broad bands with a molecular mass between 110 and 120 kDa. These bands are not detected in HEK cells transfected with vector alone, demonstrating the specificity of the antibodies for the DTDST protein. Treating homogenates of HEK cells expressing DTDST with *N*-glycosidase F to remove *N*-linked oligosaccharides results in a band \sim 80 kDa in size, which is similar to the estimated size of the core DTDST protein (1).

Figure 3 shows the pattern of immunofluorescent labeling of HEK cells expressing the wild-type and mutant DTDST proteins. No immunofluorescent staining was identified in HEK cells transfected with vector alone (data not shown). In cells transfected with wild-type *DTDST*, immunofluorescence was observed along the plasma membrane of the cell, with no cytoplasmic or nuclear staining detected (WT in Fig. 3). This is consistent with its role as a transmembrane sulfate transporter. The mutations A715V, C653S, Q454P and R279W demonstrated plasma membrane immunofluorescent staining similar to wild-type DTDST. In contrast, immunofluorescence of the G678V mutation was detected in relatively few cells and was observed only within the cytoplasm, as demonstrated by the two examples shown in Figure 3. Immunofluorescent staining was not detected in any of the cells following transfection with the Δ V340 mutation.

The preceding experiments demonstrate that four disease-causing mutations, A715V, C653S, Q454P and R279W, are expressed properly along the plasma membrane of mammalian cells but have reduced rates of transport when compared with wild-type DTDST. One possible explanation for the reduction in sulfate transport is that these mutations are expressed at a lower level than the wild-type protein. To test this, the amount of expressed mutant protein was compared with wild-type DTDST by performing immunoblots on whole homogenates of transfected HEK cells, and measuring the relative amount of expressed DTDST by scanning densitometry. The data in Figure 4 demonstrate that the amount of mutant protein in the cell homogenates is reduced for each of the mutations when compared with cells expressing wild-type DTDST. Wild-type *DTDST* and each *DTDST* mutation were co-transfected in HEK cells with a vector containing the *Rluc* reporter gene. Two days after transfection, luciferase activity was measured in the cell homogenates. There was no significant difference between luciferase activity in cells co-transfected with *Rluc* and wild-type *DTDST* when compared with cells co-transfected with *Rluc* and each *DTDST* mutation (data not shown). This demonstrates that the reduced protein expression for each of the mutations is not a result of inefficient transfection.

For two of the mutants in Figure 4 (G678V and Δ V340), very little protein was detected by immunoblots analysis.

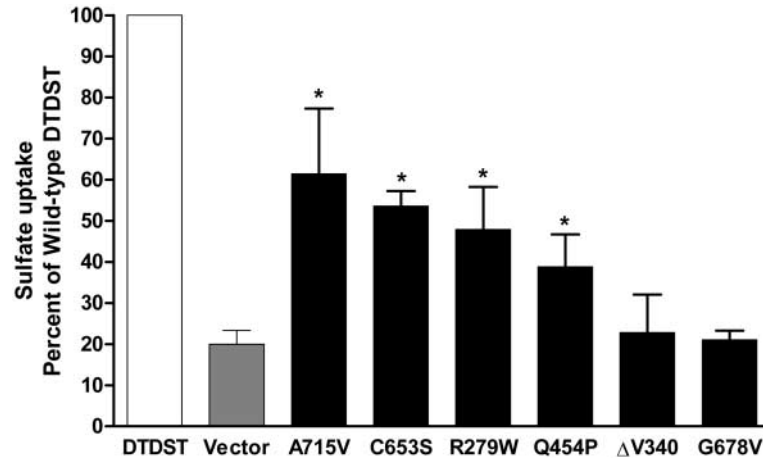


Figure 1. Sulfate uptake in HEK-293 cells transfected with wild-type *DTDST* (open bar), vector without insert (gray bar) or various *DTDST* mutations (closed bars). Each experiment represents the mean uptake of four, 35 mm plates and at least three experiments were performed for each mutation. * $P < 0.05$ compared with cells transfected with vector alone.

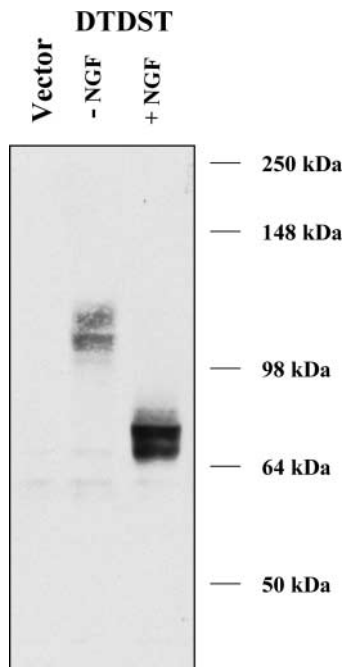


Figure 2. Expression of *DTDST* in HEK-293 cells. Each lane contains 35 μ g of solubilized HEK cell protein after transfection with either vector without insert (Vector) or with *DTDST* (second and third lanes). *DTDST*-transfected cells were treated either with (+NGF) or without (-NGF) *N*-glycosidase F. A monoclonal antibody directed against the *DTDST* protein was used to probe the immunoblots.

This is in agreement with both the lack of function observed with these two mutants in HEK cells and the minimal detection of expression by immunofluorescent microscopy. Similar results were obtained when a second anti-*DTDST* monoclonal antibody was used (data not shown), making it unlikely that the lack of expression of these two mutants is the result of alterations in the antibody recognition site. As shown in Figure 4, expression of the Q454P mutant is not only reduced when compared with wild-type *DTDST*,

but it also appears as an ~80 kDa band, which probably represents the unglycosylated form of *DTDST* (compare with Fig. 2). In examining four different immunoblots performed under conditions similar to the experiment shown in Figure 4, the amount of the Q454P mutant that is present in the unglycosylated form was variable, ranging from 50 to 100% of the expressed mutant protein.

DISCUSSION

Individuals with disease-causing mutations in the *DTDST* gene present with at least four chondrodysplasias with different levels of severity. The underlying defect in each is abnormal sulfate transport, which results in the undersulfation of cartilage proteoglycans. In a previous study, the rate of sulfate uptake by various *DTDST* mutations was determined in *X. laevis* oocytes (18). Of the 11 mutations examined in oocytes, four mutations, A715V, C653S, Q454P and G678V, had rates of sulfate transport nearly equal to that of wild-type, whereas two mutations, Δ V340 and R279W, transported sulfate at rates 17 and 32%, respectively of wild-type *DTDST*. When the sulfate transport function of the different *DTDST* mutations were grouped according to phenotypes, there were inconsistencies in terms of correlating the severity of the phenotype with the residual transport function in oocytes. For example, compound heterozygotes with a null mutation on one allele and a mutation with near-normal function in oocytes on the other allele were identified in chondrodysplasias of all levels of severity.

In general, post-translational processing is performed accurately when mammalian proteins are expressed in *X. laevis* oocytes (19); however, in some cases, mutant proteins that are functional in oocytes have been found to be non-functional in mammalian cells. This can be explained by the fact that some mutant proteins are assembled properly at the lower incubation temperatures required for *X. laevis* oocytes (17°C), but are processed abnormally at 37°C in mammalian cells (20–22).

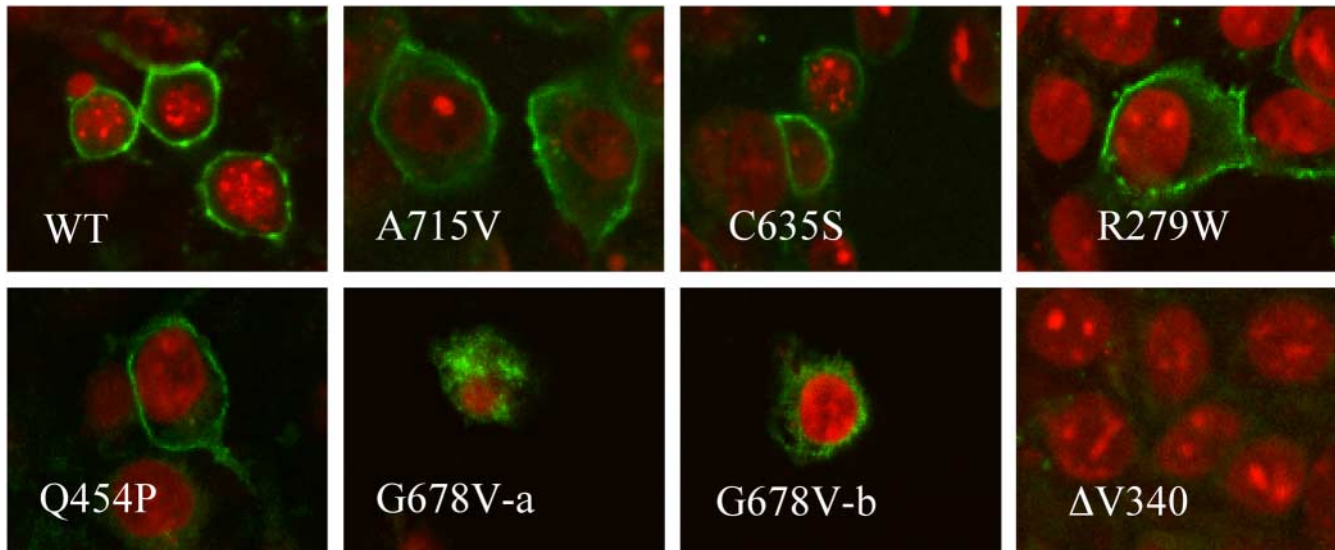


Figure 3. Confocal immunofluorescent microscopy of HEK cells transfected with either wild-type *DTDST* (WT) or various mutations. The immunofluorescent staining with an FITC-conjugated goat-anti-mouse secondary antibody labels the *DTDST* protein green. Nuclear staining was performed with ethidium bromide, which stains the nucleus red. The merged images reveal that the *DTDST* and the mutations A715V, C635S, R279W and Q454P are expressed solely along the plasma membrane and not within the cytoplasm or nucleus. Two images of the G678V mutation (G678V-a and G678V-b) show that this mutant is found within the cell cytoplasm and is not targeted to the plasma membrane. No immunofluorescent labeling of the Δ V340 mutant was detected.

To test whether the type of expression system influenced the function of *DTDST* mutations, in the present study, we transfected mammalian HEK-293 cells with six *DTDST* mutations that were shown to have partial function when expressed in oocytes (18). In contrast to the residual sulfate transport detected in oocytes for the Δ V340 and the G678V mutations, the amount of sulfate uptake in mammalian cells by these two mutations was not significantly different than that in cells transfected with vector alone. Consequently, in mammalian cells, the Δ V340 and the G678V mutations should be classified as null mutations; however, the cause of the loss of function for each of these two mutations appears to be different. In HEK cells transfected with the Δ V340 mutant, the protein is not detected by either immunoblot analysis or confocal immunofluorescent microscopy, suggesting that this mutation is either poorly expressed or the protein is rapidly degraded in mammalian cells. In contrast, the G678V mutant is detected in a few cells by immunofluorescent microscopy, but is trapped within the cell cytoplasm, most likely as a result of a defect in protein processing.

The mutations A715V, C653S, Q454P and R279W all have significant sulfate transport function when expressed in mammalian HEK cells, ranging from 39 to 62% of wild-type *DTDST* (Fig. 1); therefore, these four mutations demonstrate partial function in both *X. laevis* oocytes and mammalian cells. In addition, each of these four mutations is expressed on the cell membrane in a pattern similar to wild-type *DTDST*; however, the amount of protein expressed on the cell surface is significantly less than wild-type protein. It is unclear whether the reduced quantity of expressed protein represents decreased synthesis or increased turnover of the mutated protein.

For each mutation examined in this study, Table 1 lists the residual sulfate transport capacity according to the

chondrodysplasia in which it has been identified. In contrast to the results in oocytes, there is a strong correlation between the severity of the phenotype and the lack of sulfate transport activity in mammalian cells. For example, as seen in Table 1, a null mutation on both alleles is always found with the severe ACG-IB phenotype and never found with the less severe phenotypes. In addition, the moderately severe AO-II phenotype always has a null mutation on one allele and a partial-function mutation on the opposite allele. Interpretation of the less severe phenotypes is more complex.

Homozygotes for partial-function mutations have been described for R279W, Q454P and C653S. A recent report identified 18 individuals with rMED, who were homozygous for the R279W mutation (23). Abnormal clinical findings were present at birth only in a minority of the subjects and short stature was not a frequent finding. In another study, rMED was described in three patients homozygous for the C653S mutation (24). All three individuals had normal stature, double-layered patellae and hip dysplasia. The mild clinical presentation of individuals homozygous for either C653S or R279W is consistent with the residual transport function, proper glycosylation and plasma membrane targeting of these two mutations. On the other hand, homozygosity for the partial-function Q454P mutation has been described in a single individual, who presented with a 'broad bone-platyspondylic' variant of DTD (11). Clinical and radiographic features included macrocephaly, severe platyspondyly, malformed fingers, wide metaphyses and fibular overgrowth. It is possible that the unique features of this case are related to the fact that the Q454P mutant protein is not properly glycosylated in mammalian cells (Fig. 4).

On the basis of these observations, our data suggest that individuals with partial-function mutations on both alleles

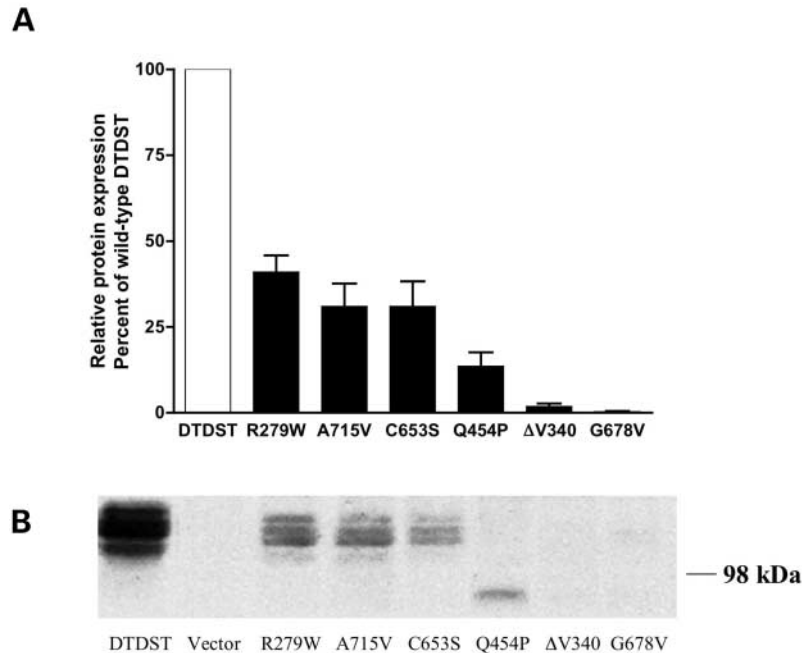


Figure 4. (A) Mutant protein expressed as a percent of wild-type DTDST. Data represent the mean \pm SE of seven scanned immunoblots. (B) Representative immunoblot with 75 μ g solubilized protein in each lane.

will present with either the mild rMED phenotype, or in the case of Q454P, a chondrodysplasia variant. Individuals with either 'classic' DTD or AO-II typically have a partial-function mutation on one allele and a loss of function mutation on the opposite allele, demonstrating that some residual sulfate transport function is required to produce either the DTD or the AO-II phenotype. This also suggests that factors other than residual sulfate transport can influence disease severity in individuals with AO-II and DTD. Similar inconsistencies have been found in other chondrodysplasias. For example, the same M202V mutation of the *FLNB* gene can result in both autosomal dominant atelosteogenesis type I and atelosteogenesis type III (25).

These general assumptions do not take into consideration the common 'Finnish' *DTDST* mutation ($DTDST_{Fin}$), which is a GT > GC transition in the splice donor site and leads to reduced levels of *DTDST* mRNA. DTD has been described with both the $DTDST_{Fin}/DTDST_{Fin}$ and the $DTDST_{Fin}/R279W$ genotypes (26,27), whereas rMED has been described in individuals with the $DTDST_{Fin}/R279W$ and the $DTDST_{Fin}/C653S$ genotypes (23). As the $DTDST_{Fin}/R279W$ genotype has been identified in both DTD and rMED, there is clearly an overlap in the phenotype with this mutation. It has been estimated that the level of correctly spliced mRNA in patients homozygous for the $DTDST_{Fin}$ mutation is \sim 5% of the wild-type allele (26); however, the amount of functional DTDST protein that is produced in the cells of these patients is unknown. As a consequence, the fact that the $DTDST_{Fin}/R279W$ genotype can result in either DTD or rMED may reflect differences in the quantity of functional protein found in these individuals.

The location of each mutation within the DTDST protein clearly influences the relative amount of residual protein

function. A715V, C653S, G678V and H665P are four known disease-causing, single amino acid substitutions found in the 3'-cytoplasmic putative STAS domain of *DTDST* (28). We tested three of these mutations and found that A715V and C653S are partial-function mutations, whereas G678V has no measurable sulfate transport activity in mammalian cells; however, the G678V mutation retains partial function when expressed in *Xenopus* oocytes. The loss of function of the G678V mutation in mammalian cells is probably due to its inability to be properly targeted to the plasma membrane. From this data, it appears that amino acid substitutions in the 3'-cytoplasmic putative STAS domain of *DTDST* can contribute to cellular sulfate uptake if the mutated protein is able to reach the plasma membrane. In contrast, the $\Delta V340$, N425D and L483P mutations are found in the predicted transmembrane domains of DTDST, whereas the R178X and the $\Delta 1751$ mutations result in premature stop codons. These types of mutations are expected to result in severe alterations in protein structure, and it is consistent with the fact that these mutations do not have significant sulfate transport function when expressed in mammalian cells.

In summary, we find that certain disease-causing mutations of the *DTDST* gene are processed differently in *Xenopus* oocytes and mammalian cells; however, in mammalian cells, there is a strong correlation between the amount of residual sulfate transport activity and the severity of the phenotype. It should be noted, that nearly 40 different mutations of the *DTDST* gene have been described, and we have examined 10 of these in mammalian cells. With the analysis of additional mutations, further insight will be gained into the structure of the DTDST protein and its relation to DTDST function and regulation.

Table 1. Functional activity of *DTDST* alleles in ACG-IB, AO-II, DTD and rMED

ACG-IB	AO-II	DTD	rMED
L483P/L483P (-/-)	R279W/ Δ a1751 (+/-)	C653S/R178X (+/-)	R279W/R279W (+/+)
Δ V340/ Δ V340 (-/-)	R279W/N425D (+/-)	R279W/ Δ V340 (+/-)	C653S/C653S (+/+)
G678V/R178X (-/-)	R279W/R178X (+/-)	Q454P/Q454P (+/+) [DTD variant]	
N425D/R178X (-/-)			

Activity: (+) partial function; (-) null mutation.

MATERIALS AND METHODS

Generation of anti-DTDST monoclonal antibodies

The preparation of the *DTDST* clone in pSPORT has been described previously (18). The *DTDST* insert, containing a C-terminal six-histidine tag, was digested from the pSPORT vector with *EcoRI* and *NotI*, and ligated into a pVL1393 baculovirus transfer vector (PharMingen). Following the expression in Sf9 cells, purification of the His-tagged DTDST protein was performed using methods described previously (29). Purified DTDST protein was concentrated by dialysis against 20% polyethylene glycol (20 000), 100 mM NaCl, 0.2% SDS, 20 mM Tris-HCl (pH 7.5) and was used as an antigen for antibody production. Hybridoma supernatants were screened against purified DTDST protein, and seven hybridomas producing anti-DTDST antibodies were selected. Immunoblots on homogenates of Sf9 cells not expressing DTDST were not different than background, confirming the specificity of the antibodies for the DTDST protein. For the majority of the studies described here, antibody I-G2 was used.

Expression in HEK-293 cells

HEK-293 cells were maintained at 37°C, 5% CO₂, and grown in Alpha Minimal Essential Media (Gibco) supplemented with 10% fetal bovine serum, 3.5 mM L-glutamine, 100 u/ml penicillin and 100 µg/ml streptomycin. Full-length human *DTDST* cDNA (minus the histidine tag) was cloned into the pcDNA3 vector (Invitrogen). The appropriate *DTDST* mutations were introduced with the Quick-Change Site-Directed Mutagenesis kit (Stratagene). The inclusion of the correct mutation was confirmed by sequence analysis. The numbering for the various nucleic acid and amino acid mutations is based on the sequence already published (1). HEK cells were transiently transfected with 4 µg cDNA/20 µl Polyfect reagent according to the manufacturer's instructions (Qiagen). For immunoblot analysis, HEK cells were cultured at 6 × 10⁵ cells per 35 mm cell culture dish and used 48 h following transfection with wild-type *DTDST*, vector alone or mutated *DTDST*. Following the treatment with trypsin for 5 min at room temperature, the cells were transferred to a 15 ml centrifuge tube, rinsed with 1 ml culture media to inactivate trypsin and centrifuged at 790g for 5 min. The cells were washed once with 5 ml phosphate buffered saline (PBS) and treated with 100 µl Complete-Mini, EDTA-free protease inhibitor (Roche). Cells were solubilized with 1% SDS in PBS and sheered through a 22 gage needle. For deglycosylation, 35 µg of solubilized HEK cell protein was treated with 50 mM 2-mercaptoethanol and boiled for 5 min. Triton X-100 was added

(0.75% v/v), and the mixture was treated with 5 U *N*-glycosidase F (Calbiochem) for 3 h at 37°C. DTDST was detected on immunoblots with anti-DTDST mouse monoclonal antibodies at a 1:400 dilution and goat, anti-mouse horseradish peroxidase-conjugated secondary antibody at a 1:20 000 dilution (Roche or Rockland). Chemiluminescence was performed with Pierce SuperSignal West. For comparison of protein expression, immunoblots containing equal amounts of solubilized protein in each lane were scanned with the Kodak Digital Science 1D program and expressed as the percent of wild-type DTDST. Transfection efficiency for each mutant was determined by co-transfection with the Promega Dual-Luciferase Reporter Assay System according to the manufacturer's instructions. Luminescence was corrected for protein concentration and expressed as the percent luminescent signal compared with cells co-transfected with wild-type *DTDST*.

Sulfate uptake in HEK cells

To measure the rate of sulfate uptake, HEK cells were cultured at 6 × 10⁵ cells per 35 mm cell culture dish and used 48 h following transfection with wild-type *DTDST*, vector alone or mutated *DTDST*. Culture medium was aspirated and each plate of cells was washed with 3 ml wash buffer (240 mM mannitol, 2.5 mM potassium sulfate, 2.8 mM calcium gluconate, 1.2 mM magnesium sulfate, and 10 mM HEPES/Tris pH 7.5) at 37°C. To initiate uptake, 1.0 ml uptake solution containing 6.0 µCi [³⁵S]sulfate/ml wash buffer was added to each plate and incubated for 1 min at 37°C. The uptake solution was aspirated and the cells rinsed twice with 3 ml wash buffer at 5°C. Cells were lysed for 1 h with 1.0 ml 1% SDS in 0.1 N sodium hydroxide. An aliquot of the lysed cells was used for protein assay (30,31), and the remainder transferred to 4 ml Biosafe II counting cocktail for scintillation spectroscopy. Sulfate uptake is expressed as DIDS-inhibited uptake per milligram protein and is calculated by subtracting sulfate uptake in the presence of 0.5 mM DIDS from sulfate uptake in the absence of DIDS. Each experiment represents the mean uptake of four, 35 mm plates for each condition tested.

Immunofluorescent confocal microscopy

HEK cells were plated at a density of 3 × 10⁵ on a Lab-Tek chamber slide pre-treated with 0.1 mg/ml poly-L-lysine, and transfected 24 h later as mentioned earlier. Forty-eight hours following transfection, the cells were washed twice with 1.0 ml PBS, incubated 5 min in 1.0 ml methanol and washed five times with 1.0 ml PBS. Subsequently, the cells were incubated for 1 h with anti-DTDST antibodies at a 1:400

dilution in 1.0 ml PBS plus 10% fetal bovine serum, washed twice with PBS, then treated with FITC-conjugated goat-anti-mouse secondary antibody (Rockland) at a 1:1000 dilution. For nuclear staining, the cells were incubated for 5 min in 1.0 ml ethidium bromide (1.0 µg/ml) and washed three times with PBS. A drop of Vectashield mounting medium is added to the chamber slide prior to placement of the coverslip. Immunofluorescent staining was visualized on a Bio-Rad 1024 confocal microscope and the images collected with LaserSharp 2000 data acquisition software and subsequently transferred to Confocal Assistant 4.02.

ACKNOWLEDGEMENTS

This work was supported in part by grant 152 from the March of Dimes Birth Defects Foundation and grant DK056718 from the National Institute of Health.

REFERENCES

- Hästbacka, J., de la Chapelle, A., Mahtani, M.M., Clines, G., Reeve-Daly, M.P., Daly, M., Hamilton, B.A., Kusumi, K., Trivedi, B., Weaver, A. *et al.* (1994) The diastrophic dysplasia gene encodes a novel sulfate transporter: positional cloning by fine-structure linkage disequilibrium mapping. *Cell*, **78**, 1073–1087.
- Satoh, H., Susaki, M., Shukunami, C., Iyama, K., Negoro, T. and Hiraki, Y. (1998) Functional analysis of diastrophic dysplasia sulfate transporter. *J. Biol. Chem.*, **273**, 12307–12315.
- Rossi, A. and Superti-Furga, A. (2001) Mutations in the diastrophic dysplasia transporter (*DTDST*) gene (SLC26A2): 22 novel mutations, mutation review, associated skeletal phenotypes and diagnostic relevance. *Hum. Mutat.*, **17**, 159–171.
- Superti-Furga, A., Hästbacka, J., Wilcox, W.R., Cohn, D.H., van der Harten, H.J., Rossi, A., Blau, N., Rimoin, D.L., Steinmann, B., Lander, E.S. and Gitzelmann, R. (1996) Achondrogenesis type IB is caused by mutations in the diastrophic dysplasia sulfate transporter gene. *Nat. Genet.*, **12**, 100–102.
- Hästbacka, J., Superti-Furga, A., Wilcox, W.R., Rimoin, D.L., Cohn, D.H. and Lander, E.S. (1996) Atelosteogenesis type II is caused by mutations in the diastrophic dysplasia sulfate transporter gene (*DTDST*): evidence for a phenotypic series involving three chondrodysplasias. *Am. J. Hum. Genet.*, **58**, 255–262.
- Lamy, M. and Maroteaux, P. (1960) Le nanisme diastrophique. *Presse Méd.*, **68**, 1976–1983.
- Walker, B.A., Scott, C.I., Hall, J.G., Murdoch, J.L. and McKusick, V.A. (1972) Diastrophic dwarfism. *Medicine*, **51**, 41–59.
- Superti-Furga, A., Neumann, L., Riebel, T., Eich, G., Steinmann, B., Spranger, J. and Kunze, J. (1999) Recessively inherited multiple epiphyseal dysplasia with normal stature, club foot, and double layered patella caused by a *DTDST* mutation. *J. Med. Genet.*, **36**, 621–624.
- Huber, C., Odent, S., Rumeur, S., Padovani, P., Penet, C., Cormier-Daire, V., Munnich, A. and Le Merrer, M. (2001) Sulphate transporter gene mutations in apparently isolated club foot. *J. Med. Genet.*, **38**, 191–193.
- Rossi, A., Bonaventure, J., Delezoide, A-L., Superti-Furga, A. and Cetta, G. (1997) Undersulfation of cartilage proteoglycans *ex vivo* and increased contribution of amino acid sulfur to sulfation *in vitro* in McAlister dysplasia/atelosteogenesis type 2. *Eur. J. Biochem.*, **248**, 741–747.
- Mégarbané, A., Haddad, F.A., Haddad-Zebouni, S., Achram, M., Eich, G., Le Merrer, M. and Superti-Furga, A. (1999) Homozygosity for a novel *DTDST* mutation in a child with a 'broad bone-platyspondylic' variant of diastrophic dysplasia. *Clin. Genet.*, **56**, 71–76.
- Superti-Furga, A., Rossi, A., Steinmann, B. and Gitzelmann, R. (1996) A chondrodysplasia family produced by mutation in the diastrophic dysplasia sulfate transporter gene: genotype/phenotype correlations. *Am. J. Med. Genet.*, **63**, 144–147.
- Superti-Furga, A. (1994) A defect in the metabolic activation of sulfate in a patient with achondrogenesis type IB. *Am. J. Hum. Genet.*, **55**, 1137–1145.
- Rossi, A., van der Harten, H.J., Beemer, F.A., Kleijer, W.J., Gitzelmann, R., Steinmann, B. and Superti-Furga, A. (1996) Phenotypic and genotypic overlap between atelosteogenesis type 2 and diastrophic dysplasia. *Hum. Genet.*, **98**, 657–661.
- Rossi, A., Kaitila, I., Wilcox, W.R., Rimoin, D.L., Steinmann, B., Cetta, G. and Superti-Furga, A. (1998) Proteoglycan sulfation in cartilage and cell cultures from patients with sulfate transporter chondrodysplasias: relationship to clinical severity and indication on the role of intracellular sulfate production. *Matrix Biol.*, **17**, 361–369.
- Rossi, A., Bonaventure, J., Delezoide, A-L., Cetta, G. and Superti-Furga, A. (1996) Undersulfation of proteoglycans synthesized by chondrocytes from a patient with achondrogenesis type IB homozygous for an L483P substitution in the diastrophic dysplasia sulfate transporter. *J. Biol. Chem.*, **271**, 18456–18464.
- Rossi, A., Cetta, G., Piazza, R., Bonaventure, J., Steinmann, B. and Superti-Furga, A. (2003) *In vitro* proteoglycan sulfation derived from sulphydryl compounds in sulfate transporter chondrodysplasias. *Ped. Path. Mol. Med.*, **22**, 311–321.
- Karniski, L.P. (2001) Mutations in the diastrophic dysplasia sulfate transporter (*DTDST*) gene: correlation between sulfate transport activity and chondrodysplasia phenotype. *Hum. Mol. Genet.*, **10**, 1485–1490.
- Sigel, E. (1990) Use of *Xenopus* oocytes for the functional expression of plasma membrane proteins. *J. Mem. Biol.*, **117**, 201–221.
- Machamer, C.E. and Rose, J.K. (1988) Vesicular stomatitis virus G proteins with altered glycosylation sites display temperature-sensitive intracellular transport and are subject to aberrant intermolecular disulfide bonding. *J. Biol. Chem.*, **263**, 5955–5960.
- Denning, G.M., Anderson, M.P., Amara, J.F., Marshall, J., Smith, A.E. and Welsh, M.J. (1992) Processing of mutant cystic fibrosis transmembrane conductance regulator is temperature-sensitive. *Nature*, **358**, 761–764.
- Baron, D., Assaraf, Y.G., Cohen, N. and Aronheim, A. (2002) Lack of plasma membrane targeting of a G172D mutant thiamine transporter derived from Rogers syndrome family. *Mol. Med.*, **8**, 462–474.
- Ballhausen, D., Bonafe, L., Terhal, P., Unger, S.L., Bellus, G., Classen, M., Hamel, B.C., Springer, J., Zabel, B., Cohn, D.H. *et al.* (2003) Recessive multiple epiphyseal dysplasia (rMED): phenotype delineation in eighteen homozygotes for *DTDST* mutation R279W. *J. Med. Genet.*, **40**, 65–71.
- Makitie, O., Savarirayan, R., Bonafe, L., Robertson, S., Susic, M., Superti-Furga, A. and Cole, W.G. (2003) Autosomal recessive multiple epiphyseal dysplasia with homozygosity for C653S in the *DTDST* gene. *Am. J. Med. Genet.*, **122A**, 187–192.
- Krakow, D., Robertson, S.P., King, L.M., Morgan, T., Sebald, E.T., Bertolotto, C., Wachsmann-Hogiu, S., Acuna, D., Shapiro, S.S., Takafuta, T. *et al.* (2004) Mutations in the gene encoding filamin B disrupt vertebral segmentation, joint formation and skeletogenesis. *Nat. Genet.*, **36**, 405–410.
- Hästbacka, J., Kerrebrock, A., Mokka, K., Clines, G., Lovett, M., Kaitila, I., de la Chapelle, A. and Lander, E.S. (1999) Identification of the Finnish founder mutation for diastrophic dysplasia (DTD). *Eur. J. Hum. Genet.*, **7**, 664–670.
- Remes, V.M., Hästbacka, J., Poussa, M.S. and Peltonen, J.I. (2002) Does genotype predict development of the spinal deformity in patients with diastrophic dysplasia? *Eur. Spine J.*, **11**, 327–331.
- Aravind, L. and Koonin, E.V. (2000) The STAS domain—a link between anion transporters and antisigma-factor antagonists. *Curr. Biol.*, **10**, R53–R55.
- Karniski, L.P., Lötscher, M., Fucntese, M., Hilfiker, H., Biber, J. and Murer, H. (1998) Immunolocalization of the sat-1 sulfate-oxalate-bicarbonate anion exchanger in the rat kidney. *Am. J. Physiol.*, **275**, F79–F87.
- Lowry, O.H., Rosebrough, N.J., Farr, A.L. and Randall, R.J. (1951) Protein measurement with the Folin phenol reagent. *J. Biol. Chem.*, **193**, 265–275.
- Peterson, G.L. (1977) A simplification of the protein assay method of Lowry *et al.* which is more generally applicable. *Anal. Biochem.*, **83**, 346–356.